Hindawi
Journal of Mathematics
Volume 2021, Article ID 9950020, 8 pages
https://doi.org/10.1155/2021/9950020

Research Article

Study of Heat Transfer in Magnesium Zinc Zirconium $MgZn_6Zr$ Alloy Suspended in Engine Oil

Saima Noor and Safyan Mukhtar

Department of Basic Sciences, Deanship of Preparatory Year, King Faisal University, Hofuf 31982, Al Ahsa, Saudi Arabia

Correspondence should be addressed to Saima Noor; snoor@kfu.edu.sa

Received 23 March 2021; Revised 19 May 2021; Accepted 13 November 2021; Published 29 November 2021

Academic Editor: Riaz Ahmad

In this paper, alloy nanoparticle $MgZn_6Zr$ will be analyzed for the first time in the flow of ferromagnetic nanofluid. The combination of two or more metallic substances is termed as alloy. In other words, alloys are a solid solution or mixture of more than one metallic substance. Thus, alloys have always distinct melting points. This means that alloys have melting ranges instead of melting points. Due to these characteristics, alloy nanoparticles are efficient for heat transfer in liquid flows. Thus, we will consider magnesium alloy $MgZn_6Zr$ which is suspended in the base fluid engine oil C_8H_{18}. The suspension will be analyzed along a dipole; thus, the fluid is known as ferromagnetic $MgZn_6Zr - C_8H_{18}$ nanofluid. Solutions will be obtained numerically through the RK-method (shooting method). Our motivation is to optimize the heat transfer through the parametric study. Further, velocity of the fluid is observed to be decreasing with increasing the volume fraction of nanoparticles while temperature profile gets a rise with increase in volume fraction. Moreover, the presence of alloys in any viscous base fluid can decline the fraction between certain fluid layers which results in fast velocity field for the proposed fluid.

1. Introduction

Nanofluids are widely used in many engineering applications ranging from the use in the mechanical industry to the medical science [1]. Usually, 90% of alloy consists of the metals present in the market place. The alloy is a metal-metal mixture or solid solution. In everyday life, bicycles, aircraft, and cooking pots are typically made up of many kinds of alloys. Solder metal, brass, sterling silver, pewter, and magnesium $MgZn_6ZrR$ are the popular and widely used alloys. Having a solid solution or combining or mixing different metals with nonmetals contributes to many benefits. Thus, combination or solid solution of metallic substances can reduce the melting points, increase hardness, and make tensile strength better. The thermal properties, i.e., heat power, density, thermal expansion, and thermal conductivity of the alloys can also be influenced by this combination or solid solution of the metallic material. This means that, due to the metallic substance mixture, the thermophysical characteristics of metals differ from the thermophysical properties of the resulting alloy. This results in the alloy having stronger thermophysical characteristics than the pure metallic material. This phenomenon therefore makes alloys effective for heat flow efficiency [2–8].

Pure metals have the characteristics of high melting point; thus, they are too soft for many uses. For instance, gold can be bend easily even at low heat. This is why gold jewelry is usually an alloy. This means that if the Curie temperature of the metals of ferrites is smaller, then the mixture of these ferrites will definitely disturb the resultant alloy. It seems from the properties of the resulting alloys that for pure metals and after taking the form of alloys, the melting point, hardness, and tensile strength vary. Similarly, along with the density, thermal expansion, thermal conductivity, and heat power of the solid solution of metal substances or alloys, the Curie temperature will also be increased. This will help the alloys in reducing friction drag and enhancing the transfer of heat. These types of characteristics of nanoparticles and the like are appropriate and applicable to all devices used for cooling or heating purposes [9–13]. Normal nanoparticles, i.e., gold, copper, aluminum, and titanium, and ferrite nanoparticles, i.e., nickel zinc ferrite, manganese zinc ferrite, and magnetite ferrite, were used by scientists and mathematicians in the history [14–17]. Due to the use of alloys for heat transfer and friction drag, this article distinguishes from all others. If the alloys of nanosized particles and base fluids are in isothermal balance, the presence of these alloys in base fluid develops the thermal properties.

As the alloys or ferrites are in isothermal equilibrium with the base fluids, thus, these alloys or ferrites are also very reactive. For examples, due larger melting point, iron is very hard and strong but its surface reacts with air moisture and easily rusts. To prevent iron from rusting, it is sufficient to cast iron as alloy, which enhances its inertness. This is why if the alloy nanosized particle $MgZn_6Zr$ is used with engine oil will definitely alter the properties of the resulting ferromagnetic nanofluids. The resultant fluid is still called ferromagnetic nanofluid since alloy particles and ferrite particles have same properties, i.e., alloy particles like ferrite particles have the property of Curie temperature, which ensures that the alloy particles at some temperatures become nonmagnetic [18–21]. Alloys are multiple metals, so these particles can do best in heat transfer in moving fluids, so the article focuses on these particles.

In most of the engineering problems, the differential equations are inherently nonlinear in nature. The exact solution for these partial differential equations is often difficult to obtain. To overcome this issue, researchers developed some novelties that can handle these nonlinear partial differential equations or convert them to more solvable form. For the said purpose, various techniques are employed. For instance, the reduction of partial differential equations to ordinary ones by using the similarity transformations is one of those. This method provides a suitable transformation that without disturbing the physics of problem gives a more reliable form of differential equations that can be handled either numerically or analytically.

The researchers identified various nanoparticles like magnetic particles as nonmagnetic particles and investigated their effect on surface friction and cooling rate or heating rate. Yet very rare literature on the study of alloy nanoparticles in moving fluids exists. In particular, the authors who studied alloys treat these particles as natural particles, which means that they treat them as nonmagnetic particles. Since alloys fulfill the properties of ferrites, the nanosized particle magnesium alloy $MgZn_6ZrZn$ is therefore studied in this article. Magnesium zinc zirconium $MgZn_6Zr$ is used because of the lower density and higher thermal conductivity. Because of the higher thermal conductivity, it can provide a very useful source for the heat transfer and temperature control in many industrial as well as physical situations. In the base fluid engine oil, C_8H_{18}, the magnesium alloy $MgZn_6Zr$ is suspended. In the presence of a dipole, the study is carried out to establish the moving fluid as a magnetic fluid. The graphical findings are discussed, and the effect of alloys on the transmission of heat is studied.

2. Mathematical Modeling

Consider a steady two-dimensional flow of an incompressible, viscous, and electrically nonconducting fluid driven by an impermeable sheet in the horizontal direction shown in Figure 1. By applying two equal and opposite forces along the horizontal direction which is taken as the x-axis, with the y-axis in a direction normal to the flow, the sheet is stretched with a velocity which is proportional to the distance from the origin. A magnetic dipole is located with its center on the y-axis at a distance S from the sheet. The engine oil C_8H_{18} and magnesium alloy $MgZn_6Zr$ are in thermal equilibrium. The external dipole is examined in the flow problem. The flow problem and its mathematical molding, i.e., the thermo-mechanical coupling are given in equations (1)–(5). The equations of interest are as follows:

$$\frac{\partial u}{\partial x} + \frac{\partial v}{\partial y}, \tag{1}$$

$$\rho_{nf}\left(u\frac{\partial u}{\partial x} + v\frac{\partial u}{\partial y}\right) = -\frac{\partial P}{\partial x} + \mu_{nf}\frac{\partial^2 u}{\partial y^2} + \mu_0 M\frac{\partial H}{\partial x}, \tag{2}$$

$$\left(\rho c_p\right)_{nf}\left(u\frac{\partial T}{\partial x} + v\frac{\partial T}{\partial y}\right) + \left(\rho c_p\right)_{nf}\mu_0 T\frac{\partial M}{\partial T}\left(u\frac{\partial H}{\partial x} + v\frac{\partial H}{\partial y}\right) = k_{nf}\frac{\partial^2 T}{\partial y^2}. \tag{3}$$

Equation (1) is the continuity equation. Equation (2) stands for the momentum equation, and Equation (3) gives the description for law of conservation of energy and provides the mathematical description for the temperature profile.

Boundary conditions are as follows:

$$\begin{aligned} u \mid_{y=0} &= Sx, \\ v \mid_{y=0} &= 0, \\ \frac{\partial T}{\partial y} \mid_{y=0} &= -h_c T, \end{aligned} \tag{4}$$

$$\begin{aligned} u\mid_{y\longrightarrow\infty} &\longrightarrow 0, \\ T\mid_{y\longrightarrow\infty} &\longrightarrow T_c. \end{aligned} \tag{5}$$

The respective thermophysical properties and expression of engine oil C_8H_{18} and magnesium alloy $MgZn_6Zr$ are given in Tables 1 and 2.

2.1. Magnetic Dipole. The presence of alloy particle in any base fluid needs a magnet to give magnetization to the internal alloy particles in the fluid. In this direction, for the flow of ferromagnetic $MgZn_6Zr - C_8H_{18}$ nanofluid, a dipole is taken at a distance l. The center of dipole is taken along vertical axis at distance l away from horizontal axis. The dipole attracts the alloys particles when the temperature is

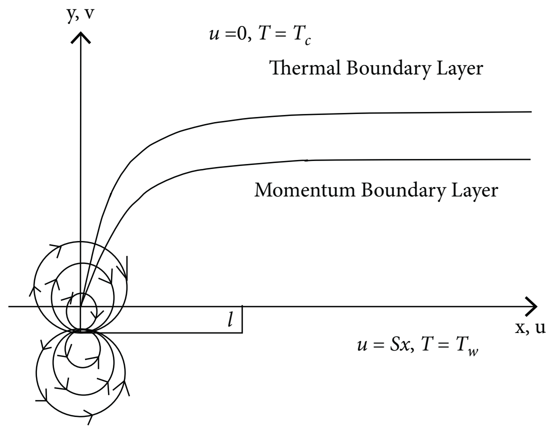

FIGURE 1: Geometry of the MgZn6Zr-C8H18 nanofluid flow.

TABLE 1: Thermophysical properties of engine oil C_8H_{18} and magnesium alloy $MgZn_6Zr$.

	ρ (kg/m^3)	C_p (J/kgK)	k (W/mK)	Pr
C_8H_{18}	890	1868	0.145	12900
$MgZn_6Zr$	2.00	960.0	120	---

TABLE 2: Thermophysical expressions of engine oil C_8H_{18} and magnesium alloy $MgZn_6Zr$.

Properties	$MgZn_6Zr - C_8H_{18}$
Viscosity μ	$\mu_{nf} = \mu_f (1-\Phi)^{-25/10}$
Density ρ	$\rho_{nf} = (1-\Phi)\rho_f + \Phi\rho_s$
Thermal conductivity k	$(k_{nf}/k_f) = (2k_f + k_s - 2\Phi(k_f - k_s)/(2k_f + k_s + \Phi(k_f - k_s)))$
Heat capacity ρC_p	$(\rho c_p)_{nf} = (1-\Phi)(\rho c_p)_f + \Phi(\rho c_p)_s$

below the Curie temperature, and for higher temperature, the alloy particles lose their magnetization. ς is given as follows:

$$\varsigma = \frac{\gamma_1}{2\pi}\frac{x}{x^2 + (y+l)^2}. \tag{6}$$

H can be defined as

$$H = \sqrt{\left(\frac{\partial\varsigma}{\partial y}\right)^2 + \left(\frac{\partial\varsigma}{\partial x}\right)^2}. \tag{7}$$

Moreover, the magnetization is taken here as follows:

$$M = K_m (T - T_\infty). \tag{8}$$

Figure 1 portrays the physical interpretation.

2.2. Similarity Analysis. Similarity variables are given as follows for the present problem:

$$\psi(\eta,\xi) = \eta\left(\frac{\mu_f}{\rho_f}\right) f(\xi),$$
$$\theta(\eta,\xi) \equiv \frac{T_c - T}{T_c} = \theta_1(\xi) + \eta^2\theta_2(\xi). \tag{9}$$

The velocity components and dimensionless coordinates are

$$\eta = x\left(\frac{\rho_f S}{\mu_f}\right)^{(1/2)},$$
$$u = \frac{\partial\psi}{\partial r} = Sxf'(\xi),$$
$$\xi = y\left(\frac{\rho_f S}{\mu_f}\right)^{(1/2)},$$
$$v = -\frac{\partial\psi}{\partial x} = -\left(S\nu_f\right)^{(1/2)} f(\xi). \tag{10}$$

These dimensionless variables transform equations (1)–(5) to equations as follows:

$$\frac{1}{(1-\Phi)^{(25/10)}A_1} f''' - (f')^2 + ff'' - \frac{2\beta\theta_1}{A_1(\xi+\gamma)^4} = 0, \tag{11}$$

$$\frac{k_{nf}}{k_f A_2}\theta_1'' + \Pr(f\theta_1' - 2f'\theta_1) + \frac{2\lambda\beta f(\theta_1 - \varepsilon)}{A_2(\xi+\gamma)^3} - \frac{4\lambda}{A_2}(f')^2 = 0, \tag{12}$$

$$\frac{k_{nf}}{k_f A_2}\theta_2'' - \Pr\left(4f'\theta_2 - f\theta_2'\right) + \frac{2\lambda\beta f\theta_2}{A_2(\xi+\gamma)^3} - \frac{\lambda\beta(\theta_1-\varepsilon)}{(\xi+\gamma)^3}\left(\frac{2f'}{(\xi+\gamma)^4} + \frac{4f}{(\xi+\gamma)^5}\right) - \frac{\lambda}{A_2}(f'')^2 = 0, \tag{13}$$

$$\begin{aligned} &f(\xi) = 0,\\ &f'(\xi) = 1,\\ &\theta_1'(\xi) = -\lambda_1\left(1+\theta_1(\xi)\right),\\ &\theta_2(\xi) = 0, \quad \text{at } \xi = 0,\\ &f'(\xi) \longrightarrow 0,\\ &\theta_1(\xi) \longrightarrow 0,\\ &\theta_2(\xi) \longrightarrow 0, \quad \text{at } \xi \longrightarrow \infty. \end{aligned} \tag{14}$$

A_1 and A_2 are

$$\begin{aligned} A_1 &= 1 - \Phi + \Phi\frac{\rho_s}{\rho_f},\\ A_2 &= 1 - \Phi + \Phi\frac{\rho c_{ps}}{\rho c_{pf}}. \end{aligned} \tag{15}$$

The parameters and dimensionless number are ε (dimensionless Curie temperature), λ (viscous dissipation), Pr (Prandtl number), λ_1 (conjugate parameter), and β (ferrohydrodynamic interaction). The mathematical representation is as follows:

$$\begin{aligned} \varepsilon &= \frac{T_\infty}{T_c},\\ \gamma &= \sqrt{\frac{S\rho_f l^2}{\mu_f}},\\ \beta &= \frac{\gamma_1}{2\pi}\frac{\mu_0 K_m T_c \rho_f}{\mu_f^2},\\ \lambda &= \frac{S\mu_f^2}{\rho_f K_m T_c},\\ \lambda_1 &= h_c\sqrt{\frac{\mu_f}{\rho_f S}},\\ \Pr &= \frac{\nu_f}{\alpha_f}. \end{aligned} \tag{16}$$

The surface friction and heat transfer rate of engineering interest are as follows:

$$\begin{aligned} C_f &= \frac{\tau_w}{(1/2)\rho_{nf}U_w^2},\\ \tau_w &= \mu_{nf}\frac{\partial u}{\partial y}\bigg|_{y=0},\\ \mathrm{Nu}_x &= \frac{xk_{nf}}{k_f(T_c - T_w)}\frac{\partial T}{\partial y}\bigg|_{y=0}. \end{aligned} \tag{17}$$

The dimensionless forms are as follows:

$$\begin{aligned} \frac{1}{2}\mathrm{Re}_x^{(1/2)}C_f &= \frac{1}{(1-\Phi)^{(25/10)}}f''(0),\\ \mathrm{Re}_x^{-(1/2)}\mathrm{Nu}_x &= \frac{-\lambda_1 k_{nf}}{k_f}\left(1 + \frac{1}{\theta_1(0) + \eta^2\theta_2(0)}\right). \end{aligned} \tag{18}$$

Here, Re_x denotes the Reynolds number that is the ratio of inertial to viscous forces; mathematically, one can write $\mathrm{Re}_x = xU_w/\nu_f$.

3. Numerical Simulation

The problem of heat transfer is simulated numerically in Matlab [22, 23]. Equations (11)–(14) are transformed to first-order differential equations and then entertained via shooting technique in Matlab. The discussion section contains its simulation and physical explanation. The procedure and its reduction to first-order equations are as follows:

$$\begin{aligned} z_1 &= f(\xi),\\ z_2 &= f'(\xi),\\ z_3 &= f''(\xi),\\ z_3' &= f'''(\xi),\\ z_4 &= \theta_1(\xi),\\ z_5 &= \theta_1'(\xi),\\ z_5' &= \theta_1''(\xi),\\ z_6 &= \theta_2(\xi),\\ z_7 &= \theta_2'(\xi),\\ z_7' &= \theta_2''(\xi). \end{aligned} \tag{19}$$

Equation (19) reduces equations (11)–(14) to the following form:

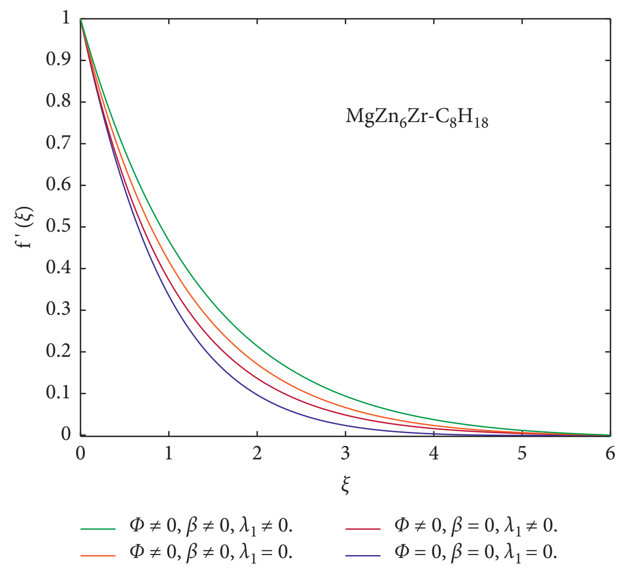

Figure 2: Comparision of velocity field in $MgZn_6Zr - C_8H_{18}$ for ferrohydrodynamic parameter, Newtonian heating, and solid volume fraction.

$$
\begin{aligned}
z_3' &= (1-\Phi)^{(25/10)} A_1\left(z_2 * z_2 - z_1 * z_3 + \frac{2\beta z_4}{A_1(\xi+\gamma)^4}\right),\\
z_5' &= -\frac{k_f A_2}{k_{nf}}\left(\Pr\left(z_1 z_5 - 2 z_2 z_4\right) + \frac{2\lambda\beta z_1\left(z_4-\varepsilon\right)}{A_2(\xi+\gamma)^3} - \frac{4\lambda}{A_2} z_2^2\right),\\
z_7' &= \frac{k_f A_2}{k_{nf}}\left(\Pr\left(4 z_2 z_6 - z_1 z_7\right) - \frac{2\lambda\beta z_1 z_6}{A_2(\xi+\gamma)^3} + \frac{\lambda}{A_2} z_2^2 + \frac{\lambda\beta\left(z_4-\varepsilon\right)}{(\xi+\gamma)^3}\left(\frac{2z_2}{(\xi+\gamma)^4} + \frac{4z_1}{(\xi+\gamma)^5}\right)\right).
\end{aligned}
\tag{20}
$$

The boundary conditions given in equation (14) take the form as follows:

$$
\begin{aligned}
z_1 &= 0,\\
z_2 &= 1,\\
z_5 &= -\lambda_1\left(1+z_4\right),\\
z_6 &= 0, \quad \text{at } \xi = 0,\\
z_2 &\longrightarrow 0,\\
z_4 &\longrightarrow 0,\\
z_6 &\longrightarrow 0, \quad \text{at } \xi \longrightarrow \infty.
\end{aligned}
\tag{21}
$$

4. Discussion

The ferromagnetic nanofluid consists of alloy $MgZn_6Zr$ with C_8H_{18} base fluid. The alloy nanoparticle in the flow analysis is taken to address what happens exactly to heat transfer when an external field is placed or removed. This analysis is incorporated only to know whether ferromagnetic $MgZn_6Zr - C_8H_{18}$ nanofluid is efficient for flow of heat; if the ferromagnetic $MgZn_6Zr - C_8H_{18}$ nanofluid performs, then the ferromagnetic $MgZn_6Zr - C_8H_{18}$ nanofluid must attract the industrial users and engineers from the fields indulging all those equipments and devices which transfer heat. The Newtonian heating is defined at the surface; this leads to help the alloy nanoparticles in transferring heat from internal side to outside the fluid. Thus, this model can be more suitable for transferring heat as compared with other studied nanoparticles or ferrite nanoparticles.

In this direction, Figures 2 and 3 are sketched to check out the impacts of alloy $MgZn_6Zr$ on velocity and temperature fields. Enhancement in axial velocity for ferromagnetic $MgZn_6Zr - C_8H_{18}$ nanofluid is examined. The ferromagnetic $MgZn_6Zr - C_8H_{18}$ nanofluid contains alloy $MgZn_6Zr$ nanoparticle as the alloy $MgZn_6Zr$ has the property of Curie temperature. Further, the base fluid and alloy have different thermophysical properties; thus, they disturb the velocity and temperature field. Thus, the variation or abrupt change in axial velocity of ferromagnetic $MgZn_6Zr - C_8H_{18}$ nanofluid is valid because of the inclusion of alloy $MgZn_6Zr$ nanoparticle; the reduction is observed for the respective cases, i.e., (i) $\Phi \neq 0$, $\beta \neq 0$, and $\lambda_1 \neq 0$. On the other hand, the low velocity in Figure 2 is evident for the ferromagnetic $MgZn_6Zr - C_8H_{18}$ nanofluid when (ii) $\Phi = 0$, $\beta \neq 0$, and $\lambda_1 \neq 0$, (iii) $\Phi \neq 0$, $\beta = 0$, and $\lambda_1 \neq 0$, and (iv) $\Phi = 0$, $\beta = 0$, and $\lambda_1 \neq 0$. This means that the presence of alloys in any viscous base fluid can decline the fraction between certain fluid layers, and as a result, one can get fast velocity field for the fluid under study. Now, the behavior

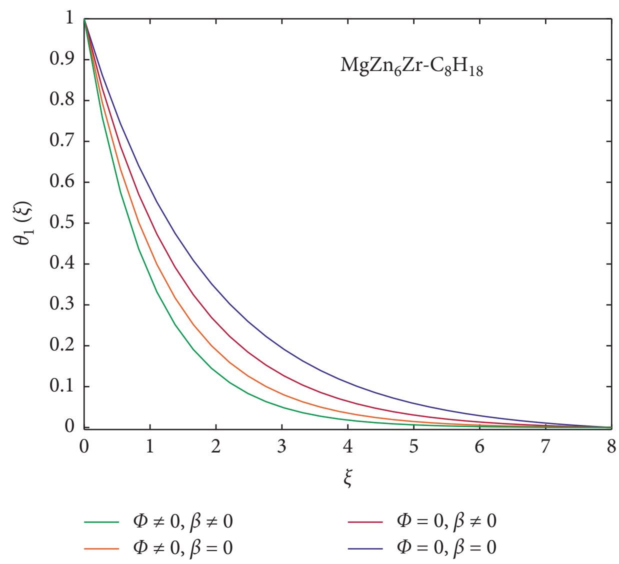

Figure 3: Comparision of temperature distribution in $MgZn_6Zr - C_8H_{18}$ for ferrohydrodynamic parameter and solid volume fraction.

of ferromagnetic $MgZn_6Zr - C_8H_{18}$ nanofluid describes that if alloy $MgZn_6Zr$ is suspended in a single base fluid, it has higher energy of transferring heat as compared with the fluids having no alloy $MgZn_6Zr$ nanoparticles. Thus, the absence of alloy $MgZn_6Zr$ leads to more resistance in the base fluids; hence, velocity declines when alloy $MgZn_6Zr$ is removed. On the other hand, temperature field in Figure 3 shows variations in ferromagnetic $MgZn_6Zr - C_8H_{18}$ nanofluid. Basically, the base fluid and alloy nanoparticle and there interaction arise the resistance; thus, the respective resistance is responsible for enhancement in temperature field. Further, the thermphysical properties of base fluid and alloy also enlarge the temperature of the flowing fluid. Here, alloy $MgZn_6Zr$ in a base fluid C_8H_{18} is suspended. This means that $MgZn_6Zr$ alloy and C_8H_{18} base fluid have different thermophysical properties in all aspects. Therefore, resulting ferromagnetic $MgZn_6Zr - C_8H_{18}$ nanofluid has different thermophysical properties and Curie temperature. Thus, the temperature field declines in the ferromagnetic $MgZn_6Zr - C_8H_{18}$ nanofluid in such a way that the highest temperature is depicted for $\Phi = 0, \beta = 0$, and $\lambda_1 \neq 0$ and decline for $\Phi \neq 0$, $\beta = 0$, and $\lambda_1 \neq 0$; $\Phi = 0$, $\beta \neq 0$, and $\lambda_1 \neq 0$; and $\Phi \neq 0$, $\beta \neq 0$, and $\lambda_1 \neq 0$.

The ferromagnetic $MgZn_6Zr - C_8H_{18}$ nanofluid is significant to compute their results and demonstrate its impacts on heat flow. The presence of alloy $MgZn_6Zr$ in a ferrofluid is analyzed for the first time. Thus, it is important to plot comparative results with a simple base fluid. In this way, the graphical results, i.e., Figures 4 and 5, delineate the hydrodynamic interaction parameter β on the fields of axial velocity and temperature. The influence of hydrodynamic interaction β on the axial velocity of ferromagnetic $MgZn_6Zr - C_8H_{18}$ nanofluid is inspected in Figure 4. The simulation of alloy $MgZn_6Zr$ in the base fluid C_8H_{18} shows that enhancement in axial velocity takes place when hydrodynamic interaction β parameter arises. Maximum enhancement is noticed for the $MgZn_6Zr - C_8H_{18}$ nanofluid, where the minimum change takes place in $MgZn_6Zr - C_8H_{18}$, when $\Phi = 0$. Giving variation to hydrodynamic interaction parameter β leads to

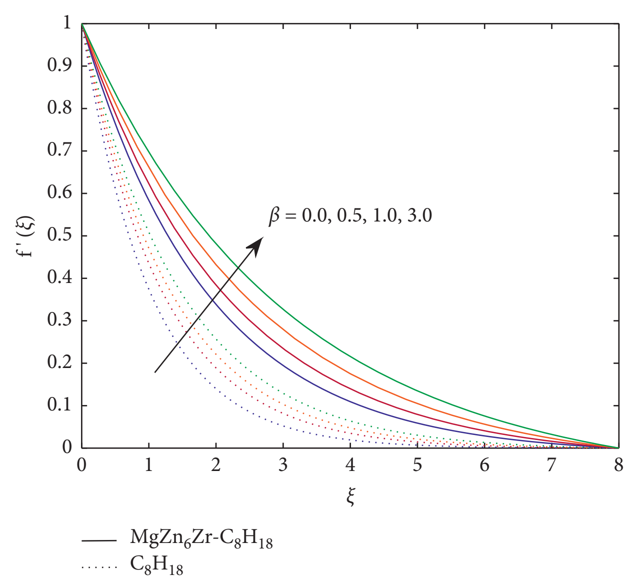

Figure 4: Axial velocity and its comparison in the flow of $MgZn_6Zr - C_8H_{18}$ and C_8H_{18} via β.

enhanced velocity of ferromagnetic $MgZn_6Zr - C_8H_{18}$ nanofluid compared with the ferromagnetic fluid, i.e., $\Phi = 0$. This happens because of the presence of alloy $MgZn_6Zr$ in the ferromagnetic $MgZn_6Zr - C_8H_{18}$ nanofluid; thus, alloy $MgZn_6Zr$ gives more attraction to the dipole. Maximum decrease in temperature distribution is described for the ferromagnetic fluid, i.e., $\Phi = 0$, as presented in Figure 5. The simulation of hydrodynamic interaction parameter means that the dipole is essential for the flow of heat if the cooling or heating agent $MgZn_6Zr - C_8H_{18}$ is used. Thus, magnetic dipole and alloy nanoparticles are significant for each other as well.

Fraction drag and heat transfer analysis is significant parameter for the analysis. Friction drag tells us what kind of resistance faces the flowing fluid in the analysis under

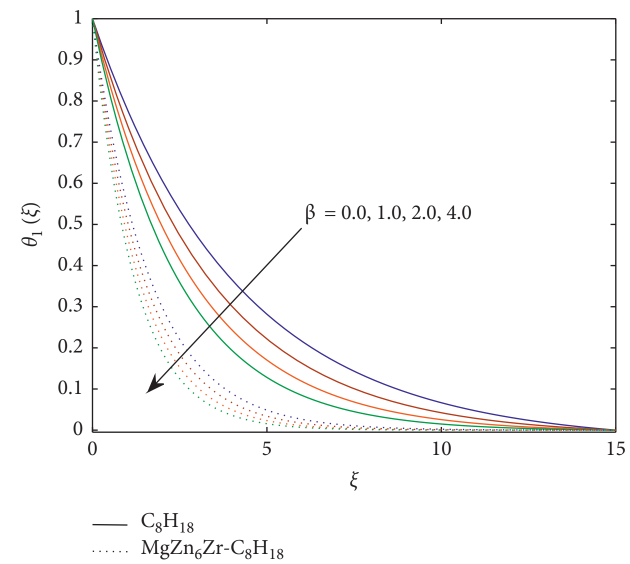

Figure 5: Temperature field in the flow of $MgZn_6Zr - C_8H_{18}$ and C_8H_{18} via β.

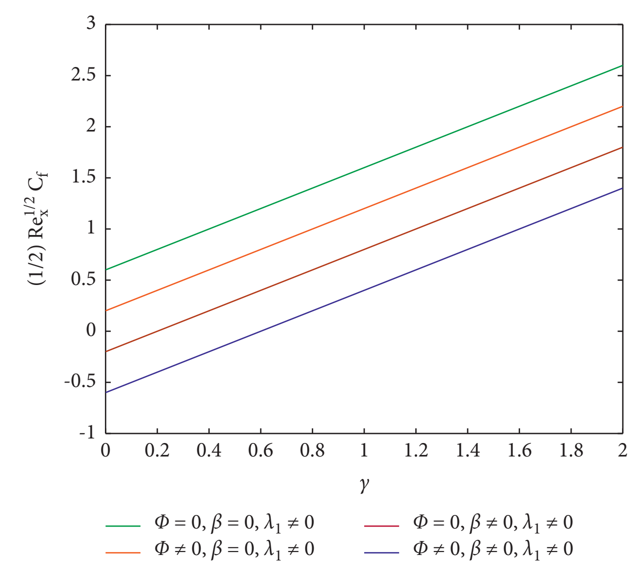

Figure 6: Different cases comparison of friction drag in the flow of $MgZn_6Zr - C_8H_{18}$ and C_8H_{18}.

discussion whereas the rate of heat flux between two points in a material is proportional to the difference in temperature between the points and the ratio of the distance between two points. Fourier's law helps in simulation of heat flow. This section includes the analysis of heat transfer flow and skin friction for the present problem. Figure 6 examines friction drag in the ferromagnetic $MgZn_6Zr - C_8H_{18}$ nanofluid. The comparison of skin friction coefficient is made for different cases, i.e., maximum resistance is described for $\Phi = 0$, $\beta = 0$, and $\lambda_1 \neq 0$ and decline for $\Phi \neq 0$, $\beta = 0$, and $\lambda_1 \neq 0$; $\Phi = 0$, $\beta \neq 0$, and $\lambda_1 \neq 0$; and lowest resistance is observed for $\Phi \neq 0$, $\beta \neq 0$, and $\lambda_1 \neq 0$. Maximum reduction in wall shear stress is demonstrated for ferromagnetic $MgZn_6Zr - C_8H_{18}$ nanofluid when $\Phi = 0$, $\beta = 0$, and $\lambda_1 \neq 0$. Figure 7 reveals that the Nusselt number arises in the flow of ferromagnetic $MgZn_6Zr - C_8H_{18}$

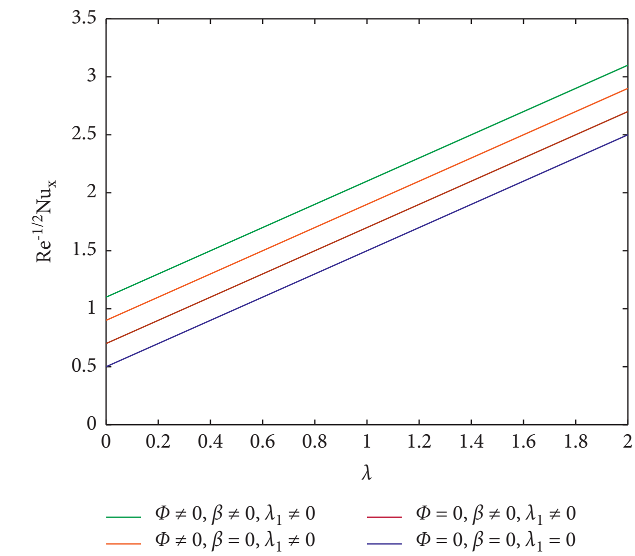

Figure 7: Different cases comparison of heat transfer rate in the flow of $MgZn_6Zr - C_8H_{18}$ and C_8H_{18}.

nanofluid, when $\Phi \neq 0$, $\beta \neq 0$, and $\lambda_1 \neq 0$; thus, the ferromagnetic $MgZn_6Zr - C_8H_{18}$ nanofluid is efficient for the heat transfer whereas the minimum heat transfer is examined for the case when $\Phi = 0$, $\beta = 0$, and $\lambda_1 \neq 0$. Physically, this means that the presence of alloy $MgZn_6Zr$ particles in the base C_8H_{18} ferrofluid really enhances the rate of heat transfer.

5. Concluding Remarks

The article discuses heat transfer for the first time in the alloy nanoparticles suspended in a ferrofluid theoretically. The analysis described in the article further studied friction drag in alloy nanoparticles. Heat transfer is needed in fluid flow that helps to reduce heat in mechanical devices. Usually, scientists use nonmagnetized particles or particles that have no Curie temperature, but when heat transfer involves a magnetic fluid, those particles become useless. The nonmagnetized particles are also useless for heat transfer. $NiZnFe_3O_4$, $MnZnFe_3O_4$, and so many others are particles satisfy the magnetization property. These mentioned particles are available in the literature. The alloys are rarely used in this direction for heat transfer; thus, the analysis is made. It is observed that alloys in any viscous base fluid might reduce the fraction between particular fluid layers, resulting in a fast velocity field for the proposed fluid. Hence, it is concluded that for heat transfer instead of viscous ferrofluid described in the results section, the presence of alloy is effective. This study can be further extended by considering variable thermophysical properties.

Abbreviations

u, v: Velocity components
μ_{nf}: Dynamic viscosity
ρ_{nf}: Density of hybrid nanofluid
P: Pressure
S: Stretching rate

Re_x: Reynolds number
C_f: Skin friction
Nu_x: Nusselt number
H: Magnetic field
$(\rho c_p)_{nf}$: Specific heat of hybrid nanofluid
k_{nf}: Thermal conductivity of hybrid nanofluid
T: Temperature
M: Magnetization
T_c: Curie temperature
K_m: Pyromagnetic coefficient
ρ_{nf}: Density of hybrid nanofluid
γ_1: Magnetic field induction
ς: Magnetic scalar potential function.

Data Availability

No data were used to support this study.

Conflicts of Interest

The authors declare that they have no conflicts of interest.

Acknowledgments

The authors are thankful to Deanship of Scientific Research, King Faisal University, for research grant through the Nasher track (206039).

References

[1] A. G. Olabi, K. Elsaid, E. T. Sayed et al., "Application of nanofluids for enhanced waste heat recovery: a review," *Nanomaterials and Energy*, vol. 84, Article ID 105871, 2021.

[2] A. Y. Fong, Y. Kodera, M. Murata et al., "Kinetics of densification/phase transformation and transport properties of Mg-Sn cubic/trigonal composites," *Materials Science and Engineering: B*, vol. 259, Article ID 114607, 2020.

[3] M. Kamran and M. Anis-ur-Rehman, "Enhanced transport properties in Ce doped cobalt ferrites nanoparticles for resistive RAM applications," *Journal of Alloys and Compounds*, vol. 822, Article ID 153583, 2020.

[4] M. Arifuzzaman and M. B. Hossen, "Effect of Cu substitution on structural and electric transport properties of Ni-Cd nanoferrites," *Results in Physics*, vol. 16, Article ID 102824, 2020.

[5] P. Naresh, A. Padmaja, and K. S. Kumar, "Influence of zinc oxide addition on the biological activity and electrical transport properties of TeO2-Li2O-B2O3 glasses," *Materialia*, vol. 9, Article ID 100575, 2020.

[6] Z. Grzesik, G. Smoła, M. Miszczak et al., "Defect structure and transport properties of (Co, Cr, Fe, Mn, Ni) 3O4 spinel-structured high entropy oxide," *Journal of the European Ceramic Society*, vol. 40, no. 3, pp. 835–839, 2020.

[7] H. H. Singh and H. B. Sharma, "Impedance spectroscopy and transport properties of polymer-based flexible nanocomposites," *Solid State Communications*, vol. 319, Article ID 114012, 2020.

[8] S. Li, X. Yang, J. Hou, and W. Du, "A review on thermal conductivity of magnesium and its alloys," *Journal of Magnesium and Alloys*, vol. 8, no. 1, pp. 78–90, 2020.

[9] L. Yan, M. Zhang, M. Wang et al., "Bioresorbable mg-based metastable nano-alloys for orthopedic fixation devices," *Journal of Nanoscience and Nanotechnology*, vol. 20, no. 3, pp. 1504–1510, 2020.

[10] J. Chen, L. Liu, and J. Deng, "Spin orbit torque-based spintronic devices using L10-ordered alloys," National University of Singapore (SG), Singapore, U.S. Patent 10, 2020.

[11] X. Liu, C. Sammarco, G. Zeng, D. Guo, W. Tang, and C.-K. Tan, "Investigations of monoclinic- and orthorhombic-based (BxGa1−x)2O3 alloys," *Applied Physics Letters*, vol. 117, no. 1, Article ID 012104, 2020.

[12] A. R. M. Siddique, K. Venkateshwar, S. Mahmud, and B. Van Heyst, "Performance analysis of bismuth-antimony-telluride-selenium alloy-based trapezoidal-shaped thermoelectric pallet for a cooling application," *Energy Conversion and Management*, vol. 222, Article ID 113245, 2020.

[13] G. K. Ramesh, S. A. Shehzad, A. Rauf, and A. J. Chamkha, "Heat transport analysis of aluminum alloy and magnetite graphene oxide through permeable cylinder with heat source/sink," *Physica Scripta*, vol. 95, no. 9, Article ID 095203, 2020.

[14] M. Gupta, V. Singh, and Z. Said, "Heat transfer analysis using zinc Ferrite/water (Hybrid) nanofluids in a circular tube: an experimental investigation and development of new correlations for thermophysical and heat transfer properties," *Sustainable Energy Technologies and Assessments*, vol. 39, Article ID 100720, 2020.

[15] K. Ajith, I. V. Muthuvijayan Enoch, A. Brusly Solomon, and A. S. Pillai, "Characterization of magnesium ferrite nanofluids for heat transfer applications," *Materials Today: Proceedings*, vol. 27, pp. 107–110, 2020.

[16] R. Kirithiga and J. Hemalatha, "Investigation of thermophysical properties of aqueous magnesium ferrite nanofluids," *Journal of Molecular Liquids*, vol. 317, Article ID 113944, 2020.

[17] M. Gupta, A. Das, S. Mohapatra, D. Das, and A. Datta, "Surfactant based synthesis and magnetic studies of cobalt ferrite," *Applied Physics A*, vol. 126, no. 8, pp. 1–13, 2020.

[18] A. Izadi, M. Siavashi, H. Rasam, and Q. Xiong, "MHD enhanced nanofluid mediated heat transfer in porous metal for CPU cooling," *Applied Thermal Engineering*, vol. 168, Article ID 114843, 2020.

[19] P. R. Jyothi Sankar, S. Venkatachalapathy, and L. G. Asirvatham, "Thermal performance enhancement studies using graphite nanofluid for heat transfer applications," *Heat Transfer*, vol. 49, no. 5, pp. 3013–3029, 2020.

[20] B. J. Fourier, *The Analytical Theory of Heat*, Cambridge University Press, London, UK, 1878.

[21] K. D. Ramaiah, G. Kotha, and K. Thangavelu, "MHD rotating flow of a Maxwell fluid with Arrhenius activation energy and non-Fourier heat flux model," *Heat Transfer*, vol. 49, no. 4, pp. 2209–2227, 2020.

[22] S. Hina, A. Shafique, and M. Mustafa, "Numerical simulations of heat transfer around a circular cylinder immersed in a shear-thinning fluid obeying Cross model," *Physica A*, vol. 540, Article ID 123184, 2003.

[23] Z. Abdelmalek, I. Khan, M. W. A. Khan, K. U. Rehman, and E. S. M. Sherif, "Computational analysis of nano-fluid due to a non-linear variable thicked stretching sheet subjected to Joule heating and thermal radiation," *Journal of Materials Research and Technology*, vol. 9, no. 5, pp. 11035–11044, 2012.